Hydrothermal synthesis of perovskite and pyrochlore powders of potassium tantalate

Gregory K.L. Goh[a)]
Materials Department and Materials Research Laboratory, University of California—Santa Barbara, Santa Barbara, California 93106

Sossina M. Haile
Materials Science Department 138-78, California Institute of Technology, 1200 California Boulevard, Pasadena, California 91125

Carlos G. Levi and Fred F. Lange
Materials Department and Materials Research Laboratory, University of California—Santa Barbara, Santa Barbara, California 93106

(Received 16 May 2002; accepted 17 September 2002)

Potassium tantalate powders were hydrothermally synthesized at 100 to 200 °C in 4 to 15 M aqueous KOH solutions. A defect pyrochlore, $KTa_2O_5(OH) \cdot nH_2O$ ($n \approx 1.4$), was obtained at 4 M KOH, but at 7–12 M KOH, this pyrochlore was gradually replaced by a defect perovskite as the stable phase. At 15 M KOH, there was no intermediate pyrochlore, only a defect perovskite, $K_{0.85}Ta_{0.92}O_{2.43}(OH)_{0.57} \cdot 0.15H_2O$. Synthesis at higher KOH concentrations led to greater incorporation of protons in the perovskite structures. The potassium vacancies required for charge compensation of incorporated protons could accommodate water molecules in the perovskite structure.

I. INTRODUCTION

The perovskite $KTaO_3$ is an incipient ferroelectric that exhibits a dielectric nonlinearity at low temperatures, on the order of the transition temperature of high-T_c superconductors. As such, a potential application is as a tunable element in microwave circuits.[1] In addition, its close lattice match with the ferroelectric $KNbO_3$ system makes it an ideal buffer layer for the growth of $KNbO_3$ films.[2] The growth of $KTaO_3$ films by the hydrothermal method was carried out and detailed in a separate study.[3] To gain a better understanding of the growth processes, potassium tantalate powders that precipitated along with the films were examined. Details of the defect and structural chemistries of these powders are the subject of the present study.

Traditionally, hydrothermal synthesis is used to produce inorganic phases at moderate temperatures (T = 400 to 700 °C) and very high pressures. Recently, it has been used for low-temperature (≤200 °C) synthesis of powders and films of several oxides, including $BaTiO_3$ and $Pb(Zr,Ti)O_3$.[4,5] In contrast, current techniques for synthesizing $KTaO_3$ powders require relatively high temperatures. Conventional solid-state synthesis based on mixed powders requires long periods of heating at 1000 °C.[6] Alternatively, when using precursors such as alkoxides, a defect pyrochlore phase, $K_2Ta_2O_6$ crystallizes at 650 °C; the perovskite phase is obtained only after heating to 850 °C.[7] Attempts to generate potassium tantalate powders by the hydrothermal method have, to date, produced materials with only a defect pyrochlore structure.[8] This paper details the first report of the hydrothermal synthesis of $KTaO_3$ powders with the perovskite structure at temperatures of 200 °C and lower.

II. EXPERIMENTAL

A series of powders was synthesized by reacting 0.0025 mol Ta_2O_5 powder in 25 ml aqueous, alkaline solutions containing 4 to 15 M KOH at 100 to 200 °C in a 45 ml Teflon-lined, stainless steel hydrothermal container (Parr Co., Moline, IL). After the reaction, the powders were filter-washed with deionized water and dried at 100 °C.

The morphology of the powders was examined with field emission scanning electron microscopy (SEM; 6300F, JEOL Ltd., Tokyo, Japan). Compositional analysis was performed by energy-dispersive spectroscopy

[a)]Address all correspondence to this author.
Present address: Institute of Materials Research and Engineering, 3 Research Link, Singapore 117602, Republic of Singapore
e-mail: g-goh@imre.org.sg

(EDS; Oxford Instruments, Oxford, United Kingdom). Phases were identified by x-ray diffraction (XRD; Philips X'pert and Philips Materials Research Diffractometer, Philips, Mahwah, NJ). The lattice parameters of the powders were determined based on peak positions for the $K_2Ta_2O_6$ (800) and $KTaO_3$ (400) phases reported in the literature,[9,10] using the silicon (400) and (511) peaks respectively, as external standards. *In situ* XRD measurements were performed in vacuum (3×10^{-4} torr) from room temperature to 320 °C using a hot stage with the Philips X'pert diffractometer.

The presence of protons in the powders was determined by ^1H magic-angle spinning nuclear magnetic resonance (MAS NMR, 12 kHz spinning rate) on a DSX 500 spectrometer (Bruker, Germany) at room temperature (25 °C) with an external tetra-methyl-silane reference. The presence of water in the powders was determined by Fourier transformed infrared (FTIR) spectroscopy (Magna IR 850 Series II, Nicolet, Madison, WI). For FTIR, powders were diluted to about 1 wt% within KBr, and this mixture was heated at 130 °C in a vacuum oven for at least 4 h to remove excess surface water before analysis in dry nitrogen at room temperature. Each spectrum collected (400–4000 cm^{-1}) was the average of 64 measurements at 4 cm^{-1} resolution. Thermogravimetric analyses (TGA/sDTA 851e, Mettler, Toledo, OH) coupled with mass spectrometry; ThermoStar, Pfeiffer Vacuum, Nashua, NH) were carried out to quantify the water content of the powders. The cycle involved heating about 30 mg of powder at 10 °C/min to 900 °C in a dry nitrogen atmosphere.

III. RESULTS

A. General observations

The XRD spectra in Fig. 1 show that synthesis at 200 °C in 7 M KOH yields a pyrochlore as an intermediate product prior to the evolution of a perovskite phase. The pyrochlore powder synthesized after 2 h had a lattice parameter of 10.623 Å, significantly larger than the value of 10.5961 Å for $K_2Ta_2O_6$ reported in the literature.[9] The perovskite structure obtained from the same solution after 24 h was cubic and had a lattice parameter of 3.991 Å, which agrees quite well with the literature value of 3.989 Å for $KTaO_3$.[10] As shown in Fig. 2, the pyrochlore and perovskite particles exhibited distinctly different morphologies—octahedral and cubic, respectively. The K/Ta ratios of the pyrochlore and perovskite phases, determined by EDS were 0.51 and 0.93, respectively, both less than their expected stoichiometry of 1.0.

Table I shows the different phases present in the powders synthesized at different temperatures and KOH concentrations; the perovskite was the only phase observed at higher temperatures and higher KOH concentrations

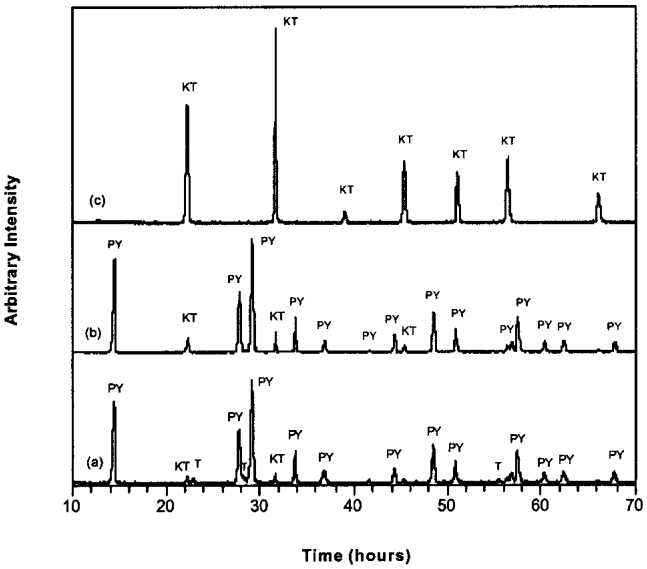

FIG. 1. XRD patterns of powders synthesized at 200 °C in 7 M KOH after (a) 2 h, primarily PY; (b) 4 h, primarily PY with increased quantity of KT; (c) 24 h, entirely KT (KT, $KTaO_3$; PY, pyrochlore; T, Ta_2O_5).

and after long reaction periods. Notably, synthesis in 15 M KOH (as observed at temperatures and time intervals reported in Table I) yielded the perovskite without evidence of the intermediate pyrochlore phase. The perovskite powders produced at this high KOH concentration at 150 and 200 °C were determined to have an increased lattice parameter of 4.000 Å. Also, the 15 M/150 °C powder had a K/Ta ratio of 0.93, and the particles were cubic in shape but smaller and more uniform in size than the perovskite particles synthesized at 7 M KOH [see Figs. 2(b) and 2(c)].

When a solution of 7 M KOH and 8 M CsOH (this yielded an OH^- concentration of 15 M while keeping the K^+ concentration at 7 M) was used at a processing temperature of 150 °C, no intermediate pyrochlore was observed, although the perovskite phase was still obtained, similar to the case when only 15 M KOH is used (see Table I, 150 °C, 15 M KOH). Conversely, only pyrochlore was present after 16 h when the synthesis was performed at 200 °C and 4 M KOH. (This powder had octahedral particles, a lattice parameter of 10.619 Å, and a K/Ta ratio of 0.46.) These observations suggest that the hydroxyl ion concentration was the critical parameter promoting the formation of the pyrochlore phase.

B. Perovskite powders

FTIR spectroscopy shown in Fig. 3 for perovskite powders synthesized at 7 M/200 °C/24 h and 15 M/150 °C/4 h, hereafter referred to as the 7 M and 15 M perovskite powders, respectively, revealed a broad band from 2800 to 3700 cm^{-1}. This broadness is

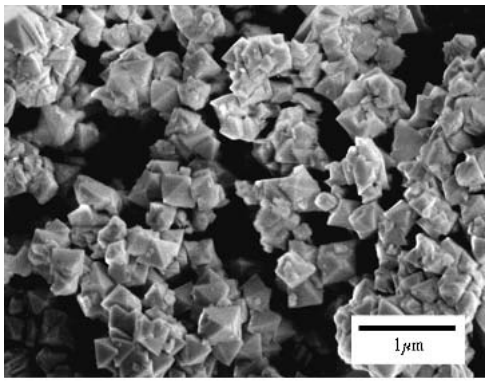

(a)

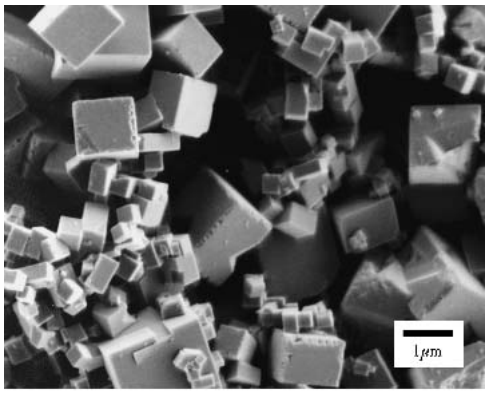

(b)

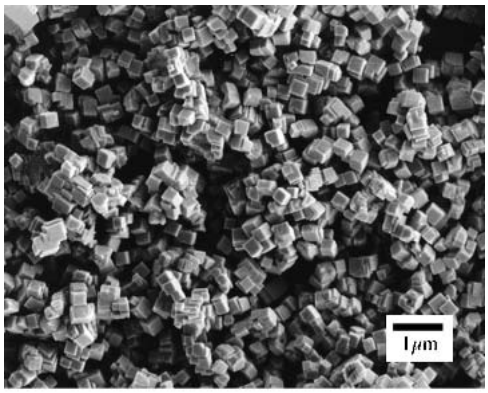

(c)

FIG. 2. SEM micrographs of (a) pyrochlore powder synthesized at 7 M/200 °C after 2 h, (b) perovskite powder synthesized at 7 M/200 °C after 24 h, and (c) perovskite powder synthesized at 15 M/150 °C after 4 h.

normally ascribed to the overlap of O–H stretching vibrations of hydroxyl groups and water molecules. In comparison with the O–H stretching band, the band at approximately 1650 cm^{-1}, ascribed to the bending vibration of H_2O, was relatively less significant for both powders. ^1H MAS NMR data shown in Fig. 4(a) revealed only one significant peak at 5.47 ppm for the 7 M perovskite powder and similarly at 5.46 ppm for the 15 M perovskite powder (latter not shown). The magnitude of the shift is typical of that observed for internally incorporated protons (as opposed to surface H_2O or surface hydroxyl groups) with OH^- stretching frequencies around 3400 cm^{-1}.[11] The total integrated ^1H MAS NMR signal for the 15 M perovskite powder was 4.2 times that for the 7 M perovskite powder on a per gram basis.

Mass spectrometry assisted TGA data shown in Fig. 5 taken between room temperature and 900 °C revealed a total weight loss of 0.68 wt% for the 7 M perovskite powder and 3.1 wt% for the 15 M perovskite powder, 4.6 times greater than the former. In both cases, mass spectrometry ascribed the weight loss to the evolution of water. This agrees quite well with earlier observations by ^1H NMR that the concentration of internally incorporated protons for the 15 M powder was 4.2 times greater than that for the 7 M powder. Also, approximately 68% of the weight loss occurred before 350 °C for the 15 M perovskite powder, compared with only 33% for the 7 M perovskite powder. After the TGA treatment, XRD showed that the lattice parameter of the 15 M perovskite powder had decreased from 4.000 to 3.992 Å, similar to the one observed in the as-synthesized condition for the 7 M powder and close to the theoretical value of 3.989 Å, as noted in Sec. III. A.

C. Pyrochlore powders

Figure 6 shows the FTIR spectrum for the pyrochlore powder synthesized at 4 M/200 °C/16 h; it also exhibits the broad O–H stretching band at 2800 to 3700 cm^{-1}. In contrast to the perovskite powders, the band at 1635 cm^{-1} characteristic of the bending mode of H_2O was more significant. The spectrum for the material synthesized at 7 M/200 °C/2 h, containing primarily pyrochlore, was similar, consistent with the presence of H_2O and hydroxyl groups. The ^1H MAS NMR spectra for the 4 M pyrochlore powder, shown in Fig. 4(b), had two peaks, indicating the presence of at least two types of protons incorporated into the structure.

The TGA data in Fig. 7 for the pyrochlore powders showed that all measurable weight loss occurred below 450 °C. The total weight loss for the 4 M pyrochlore powder was 6.45 wt% while that for the 7 M pyrochlore powder was 6.60 wt%. Concurrent mass spectrometry confirmed that these weight losses were associated with the evolution of water.

In situ hot stage XRD (3×10^{-4} torr vacuum) of the 4 M powder showed that there was a decrease in lattice parameter between 100 and 200 °C [Fig. 8(a)]. The contracted lattice was retained upon heating to 320 °C and also after cooling to room temperature. Interestingly, the lattice appeared to have expanded back to its original dimensions after the powder was exposed to laboratory air overnight (≈18 h). *In situ* hot stage XRD for the 7 M pyrochlore [Fig. 8(b)] showed that the pyrochlore lattice

TABLE I. Phases present after different processing temperatures and KOH concentrations.

Temperature (°C)	Concentration (M)	2 h	4 h	8 h	16 h	24 h	48 h
100	7				T, PY		
	15		T, KT		T, KT		
150	7		T, PY		T, PY, KT		PY, KT
	10	T, PY					PY, KT
	12	T, PY					PY, KT
	15	T, KT	KT				
175	7		T, PY, KT	PY, KT	PY, KT		PY, KT
	4		T, PY	PY	PY		
200	7	T, PY, KT	T, PY, KT	PY, KT	PY, KT	KT	
	15		KT				

Key: T, Ta_2O_5; KT, $KTaO_3$; PY, Pyrochlore; Blanks, no data collected.

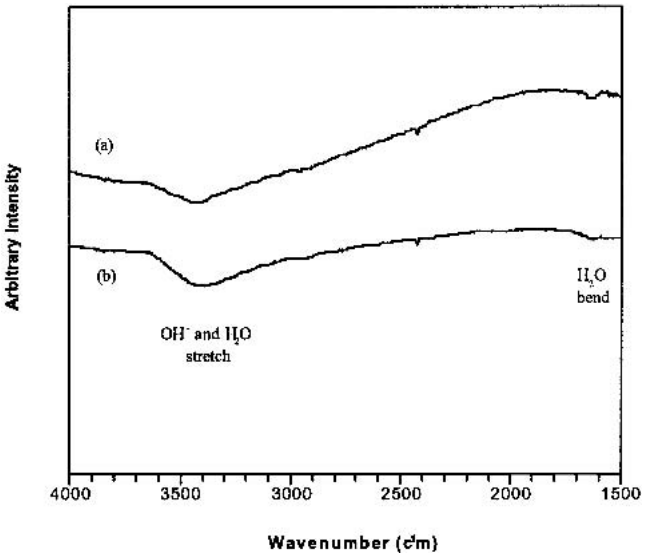

FIG. 3. FTIR spectra for perovskite powders synthesized (a) at 200 °C in 7 M KOH for 24 h, and (b) at 150 °C in 15 M KOH after 4 h.

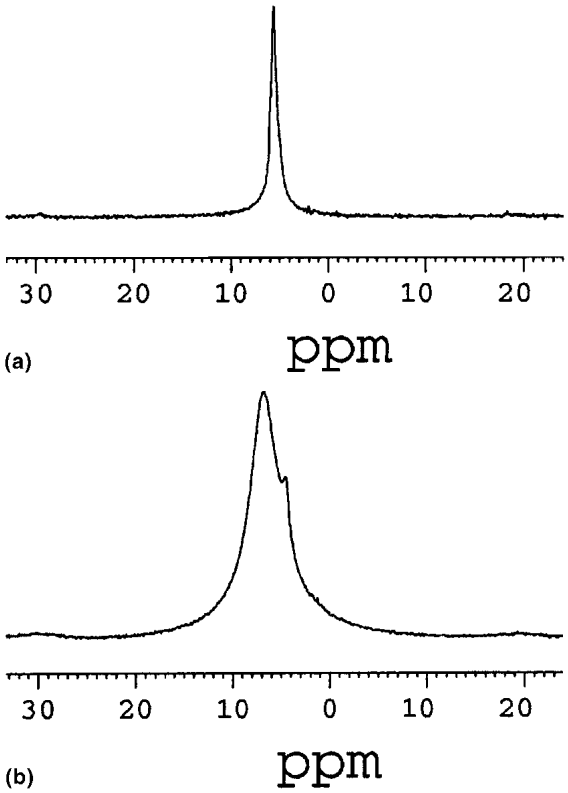

FIG. 4. ^1H NMR spectra for (a) perovskite powder synthesized at 200 °C in 7 M KOH for 24 h, and (b) pyrochlore powder synthesized at 200 °C in 4 M KOH after 16 h.

began contracting at 100 °C. Like the 4 M powder, the contracted lattice was retained after cooling from 320 °C to room temperature but expanded back to its original volume after the 7 M powder was exposed to air overnight.

IV. DISCUSSION

A. Perovskite powders

The high degree of K/Ta nonstoichiometry and proton incorporation observed for the perovskite powders has implications for the defect chemistry and dehydration mechanism. The protons may be present either in the form of hydroxyl groups (residing on sites normally occupied by oxygen atoms) or as H_2O molecules (residing in currently unspecified locations). The former is common for many perovskites and has, for example, been observed for potassium tantalate perovskite crystals grown from the melt.[12] To account for these two possible modes of proton incorporation and the cation vacancies that likely accompany hydroxyl group formation,[13–16] the chemical formula of potassium tantalate hydrate may be written as $K_xTa_yO_{3-z}(OH)_z \cdot nH_2O$, where $x + 5y + z = 6$ is required for overall charge neutrality. The presence of cation vacancies as charge compensation defects is experimentally supported by the work of Shi and coworkers,[6] who observed by FTIR and electron paramagnetic resonance that the concentration of Ba^{2+} vacancies increased with increasing OH^- concentration in $BaTiO_3$.

Subsequent to synthesis, complete dehydration, as recorded in the TGA experiments, involves the loss of $(z/2 + n)$ molecules of water, i.e.,

$$K_xTa_yO_{3-z}(OH)_z \cdot nH_2O \rightarrow K_xTa_yO_{3-z/2} + (z/2 + n)H_2O \quad . \tag{1}$$

Thus, the magnitude of the weight loss provides useful data in helping to establish the defect chemistry.

To set the boundaries on the concentration of cation vacancies in the perovskite powders, two limiting cases will be considered. In case 1, cation vacancies are taken to be present on both potassium and tantalum sites, the K/Ta ratio is given by the chemical analysis (that is, $x = 0.93y$), and all protons are taken to be incorporated in the form of hydroxyl groups such that $n = 0$. In case 2, cation vacancies are allowed only on potassium sites, such that $y = 1$ and $x = 0.93$, but both hydroxyl groups and water molecules contribute to proton incorporation. Using these boundary conditions, the charge neutrality condition, and the value of $(z/2 + n)$ implied by the weight loss measurements, all the stoichiometric parameters can be determined. The results for both cases for the 7 M and 15 M perovskite powders are summarized in Table II. Also given is the concentration of oxygen vacancies generated during dehydration for the two cases.

To establish which of these two cases more closely reflects the physical reality, we consider the NMR and FTIR results and the plausibility of the implied defect concentrations. The NMR spectra (Fig. 4) for both perovskite powders exhibited only one peak, and this result is consistent with the presence of a single type of proton, whereas the FTIR results (Fig. 3) showing a very weak H_2O bending band suggest this proton exists in the form of OH^- rather than H_2O. Thus, both sets of results are consistent with case 1 for both perovskite powders. The type and concentration of defects implied by case 1 are quite plausible for the perovskite powder synthesized under 7 M KOH, but not for the powder synthesized under 15 M KOH. Specifically, case 1 implies a 9% vacancy concentration on the K sites and a 2% vacancy concentration on the Ta sites for the 7 M perovskite powder. In contrast, the implied vacancy concentrations are 19% and 13%, respectively, for the 15 M perovskite powder (assuming case 1). It is likely that potassium tantalate can tolerate high concentrations of potassium (A site) vacancies while maintaining the perovskite structure, as implied by the existence of $HTaO_3$. This compound, like the perovskite, is composed of a ReO_3-type cubic framework of corner sharing TaO_6

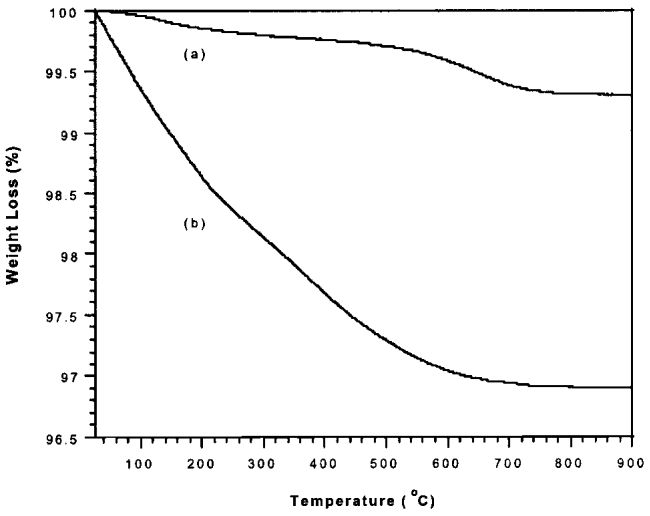

FIG. 5. TG curves for perovskite powders synthesized at (a) 7 M KOH/200 °C (24 h) and (b) 15 M KOH/150 °C (4 h).

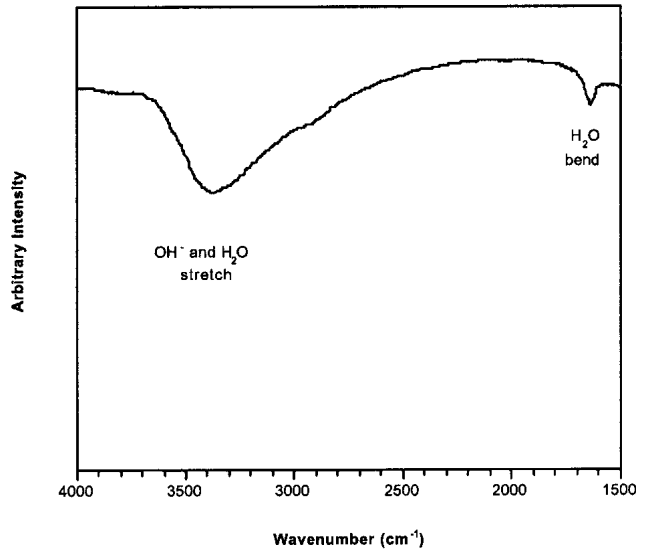

FIG. 6. FTIR spectra for pyrochlore powders synthesized at 200 °C in 4 M KOH after 16 h.

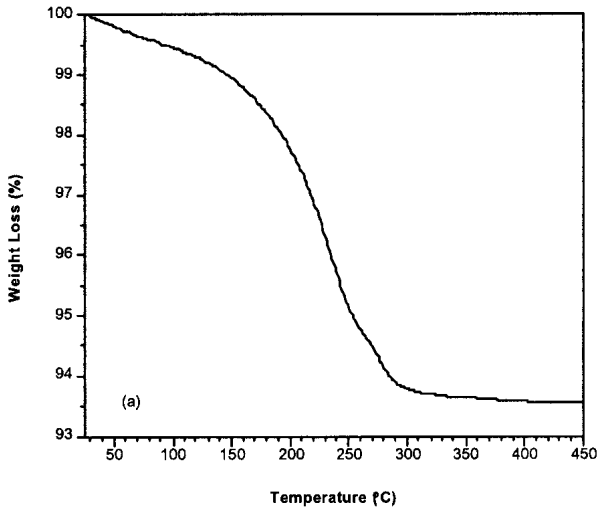

FIG. 7. TG curve for pyrochlore powder synthesized at 200 °C in 4 M KOH after 16 h.

[or $Ta(O,OH)_6$] octahedra but differs in that the perovskite A sites are completely vacant.[17] On the other hand, it is not clear if the perovskite framework can be maintained in the presence of B site vacancy concentrations as high as 13% (case 1, 15 M perovskite powder). Therefore, while case 1 is suitable for describing completely the defect chemistry of the 7 M perovskite powder, it is improbable for the 15 M perovskite powder.

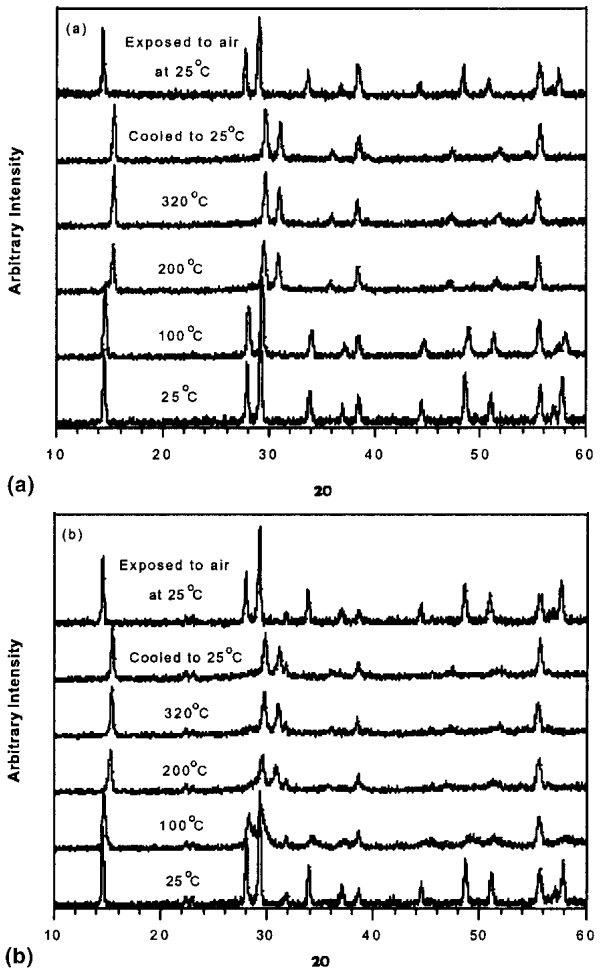

FIG. 8. *In situ* hot stage XRD (3×10^{-4} torr vacuum) patterns for pyrochlore powders (a) 4 M and (b) 7 M (the peaks at $2\theta \approx 38.5°$ and 55.5° are from the tantalum specimen holder).

TABLE II. Experimental results and defect concentrations for perovskite powders.

Synthesis conditions	7 M/24 h/200 °C	15 M/4 h/150 °C
K/Ta ratio	0.93	0.93
Lattice parameter	3.991 Å	4.000 Å
Weight loss (fraction)	0.0068	0.031
Case 1 (only OH^-, $n = 0$)		
K occupancy, x	0.91	0.81
Ta occupancy, y	0.98	0.87
OH^- per $KTaO_3$ unit, z	0.19	0.82
Fraction of O sites vacant	0.032	0.14
Case 2 (full Ta occupancy)		
K occupancy, x	0.93	0.93
OH^- per $KTaO_3$ unit, z	0.07	0.07
H_2O per $KTaO_3$ unit, n	0.066	0.44
Fraction of O sites vacant	0.012	0.012

In considering the alternative, case 2, it is necessary to establish where the H_2O molecules might reside within the perovskite structure. Given the charge neutrality of the water molecule, this species is equally likely to occupy a site normally filled by either anions or cations; it is proposed that any H_2O resides on the A (or potassium) sites, based primarily on the similarity in size of K and H_2O. This location of the water molecule can be reconciled with the NMR results, in which a single type of proton environment was revealed. The protons within potassium tantalate, as with any oxide material, will participate in the formation of hydrogen bonds between two neighboring oxygen atoms, and the chemical shift of the NMR signal is primarily established by the distance between those two oxygen atoms.[11] In the case of OH^- protons, in which the hydroxyl group resides on a normal oxide ion site, the nearest oxygen atom is at a distance of $a/\sqrt{2}$ Å (where a is the lattice parameter). This distance is also precisely the K–O distance, and a similar hydrogen bond can be formed between H_2O located on a potassium site and its nearest oxygen neighbor. Thus, the two different species, OH^- and H_2O, can produce similar local environments for the protons and thereby result in the presence of only one peak in the NMR spectra.

In the extreme of case 2, the concentration of potassium vacancies implied is 7% (for both powders). While this value is sufficient to accommodate all of the water molecules of the 7 M perovskite powder ($n = 0.066$) it is far less than what is required to accommodate all of the water molecules of the 15 M perovskite powder, for which $n = 0.44$. Thus, it is impossible for case 2 to adequately describe the defect chemistry of the 15 M perovskite powder. In light of the discussion above, we conclude that the scenario for the 15 M perovskite powder is between cases 1 and 2, and that the structure contains both potassium and tantalum vacancies as well as hydroxyl groups and water molecules (limited to the fraction of potassium vacancies, i.e., $n = 1 - x$). An estimate of the defect concentrations in this intermediate case can be established for the experimental conditions (K/Ta ratio = 0.93, dehydrated water loss of 3.1%) for the condition where $x = 0.85$, $y = 0.92$, and $z = 0.57$, namely, a dehydrated formula of $K_{0.85}Ta_{0.92}O_{2.72}$.

In addition to the two hydrogen containing species, OH^- groups on oxygen sites and H_2O molecules on potassium sites, one can also consider the possibility of proton incorporation via H_3O^+ groups, presumably also on potassium ion sites. From local charge balance considerations, such species are, perhaps, more plausible than H_2O on K sites. However, hydronium ions would be

indistinguishable from hydroxyl groups in terms of both the dehydration reaction (1) and the NMR spectra, as discussed earlier. Thus, it is impossible to establish from the experiments carried out here, whether or not they exist in potassium niobate. In any case, their presence would not change the overall balance between the concentration of K, Nb, and O atoms required for consistency with the EDS and TGA data. We note, however, that the presence of hydronium ions is more likely for the 15 M perovskite than for the 7 M material because of the greater weight loss in the former.

In all, our analysis indicates that the concentration of defects is significantly greater in the 15 M perovskite powder than in the 7 M. The 15 M perovskite powder also has the larger lattice constant, 4.000 Å, as compared to 3.991 Å. This result is consistent with observations for hydrothermally synthesized $BaTiO_3$ powders that the lattice parameter increases with increasing concentration of point defects like cation vacancies and hydroxyl groups.[16,18] It has been proposed that these defects reduce the Coulomb attractive forces between the ions, leading to an expansion of the lattice.

The dehydration reaction [reaction (1)] involves both the loss of molecular water and water present in the form of hydroxyl groups. For the case of the loss of hydroxyl groups, oxygen vacancies are generated for charge compensation, as implied above, and stated more explicitly according to[14,15]

$$2(OH_o^{\bullet}) \Leftrightarrow V_o^{\bullet\bullet} + O_o + H_2O \quad . \qquad (2)$$

The removal of the hydroxyl groups from the interior of the structure requires the concurrent diffusion of oxygen ions and protons. For undoped perovskites, oxygen is sufficiently mobile only above 600 °C.[19] For the protonic conductor, barium zirconate, which is deliberately doped to produce oxygen vacancies, the onset of dehydration is reported to occur at lower temperatures, i.e., between 350 to 550 °C.[20] In contrast, for the perovskite powders studied here, 68% and 33% of the weight loss for the 15 M and 7 M perovskite powders, respectively, occur below 350 °C. This occurs despite the fact that all oxygen sites in the hydrated perovskite [e.g., $K_{0.85}Ta_{0.92}O_{2.43}(OH)_{0.57} \cdot 0.15H_2O$] are expected to be filled with oxygen or hydroxyl ions while the potassium sites are filled with potassium ions or water molecules. As the perovskite structure is a cubic close-packed structure composed of potassium and oxygen ions, this implies that there is no path for the diffusion of water molecules out of the structure.

To account for the rapid loss of water at low temperatures, it is proposed that water molecules that sit on potassium sites at the surface are lost first. In addition, reaction (2) taking place at the surface leads to the generation and loss of additional water molecules. These two processes create the required vacant sites for the subsequent diffusion of water molecules from beneath the surface. The boundary between the region close to the surface that contains vacant potassium and oxygen sites and the interior region with hydroxyl groups and potassium sites filled with water molecules then moves progressively inward, analogous to a drying front, as water molecules diffuse to the surface. Note that reaction (2) can also take place internally near a vacant potassium site. In addition, since the water molecule is a neutral species with a Coulombic radius of 1.37 Å,[21] the molecule could diffuse to the surface by hopping through either the vacant potassium sites ($r = 1.60$ Å)[22] or the vacant oxygen sites (radius, $r = 1.42$ Å).

B. Pyrochlore powders

The general formula for a normal pyrochlore can be written as $A_2B_2O_6O'$ with four crystallographically nonequivalent atom sites; the structure can be viewed as interpenetrating networks of B_2O_6 and A_2O'.[23] In this description, the B_2O_6 network is made up of a three-dimensional array of corner-shared BO_6 octahedra interpenetrated by zig-zag chains of A_2O'. As it is the B_2O_6 network that is essential for stabilization of the structure, vacancies can exist at both A and O′ sites without changing the basic framework.[23] Vacancies at the cation and/or anion sites give rise to the defect pyrochlore structures of $A_2B_2O_6\square'$ or $A\square B_2O_6\square'$, [24,25] many of which are found hydrated.[8,24,26–29]

As the K/Ta ratio of the pyrochlore phase found in this study is ≈0.5, its structure appears to be of the second type, $A\square B_2O_6\square'$. Duan and co-workers, who also synthesized the pyrochlore phase at 4.4 M KOH/200 °C/48 h and also observed a K/Ta ratio of ≈0.5, proposed that one of the oxygen atoms in the B_2O_6 unit is substituted by a hydroxyl ion and furthermore that the compound is hydrated, thereby giving a formula of $K\square Ta_2O_5(OH)\square \cdot nH_2O$, where □ depicts the two sites that might be occupied by the water molecules. The ^{1}H MAS NMR spectra for the 4 M pyrochlore powder synthesized in this study, shown in Fig. 4(b), indicates the presence of at least two types of protons in the structure and provides support for such a formula. In addition, FTIR studies (Fig. 6) confirm the presence of water and hydroxyl groups. When K/Ta = 0.5 is assumed for simplicity and

$$K\square Ta_2O_5(OH)\square \cdot nH_2O \rightarrow K\square Ta_2O_{5.5}\square + (n + 0.5)H_2O \quad , \qquad (3)$$

a value of $n = 1.4$ is calculated for the measured weight change (≈6.5%). This amount of water can be accommodated in the vacant potassium and oxygen sites denoted by □.

The appearance of the perovskite rather than pyrochlore phase at high OH^- concentrations is noteworthy. Neglecting for the moment the water of hydration, one could write the hydrothermal reaction as

$$Ta_2O_5 + KOH \rightarrow KTa_2O_5(OH) \text{ (defect pyrochlore)} \quad , \quad (4)$$

which then further reacts at high OH^- concentrations to form the perovskite phase

$$KTa_2O_5(OH) + KOH \rightarrow 2KTaO_3 \text{ (perovskite)} + H_2O \quad . \quad (5)$$

At lower OH^- concentrations (e.g., 4 M KOH) the 1:2 pyrochlore appears to be the only stable phase (the potassium concentration does not appear to be controlling since the perovskite phase was produced when substantial amounts of KOH were replaced by CsOH). At high OH^- concentrations, the pyrochlore is only an intermediate phase [via reaction (4)], and the perovskite is the stable phase [formed via reaction (5)].

For the K/Ta ratio to increase from the 0.51 for the pyrochlore powder to 0.93 observed for the perovskite powder, it is most likely that the conversion occurs via a dissolution–reprecipitation mechanism. A consequence of this is that even after all the precursor Ta_2O_5 powder has dissolved, soluble tantalum oxide species continue to be supplied from the dissolution of the pyrochlore. As such, it is probable that nucleation occurs over an extended period of time, concurrent with growth, leading to the larger particle size distribution observed for the 7 M perovskite powders. Following similar reasoning, it is then probable that the nucleation of the 15 M perovskite powder occurs over a much shorter period of time since its synthesis does not involve an intermediate pyrochlore, and this leads to the narrower particle size distribution observed [compare Figs. 2(b) and 2(c)].

The ease with which water can diffuse into and out of $K\square Ta_2O_5(OH)\square \cdot nH_2O$ can be understood in terms of its structure, which is permeated by three-dimensional tunnels (associated with the vacancies $\square$ on both the cation and anion sites). This defect pyrochlore is known as an octahedral molecular sieve, so named because the basic building block is a TaO_6 octahedron instead of the tetrahedra found in zeolite molecular sieves.[8] XRD, neutron diffraction, and NMR experiments on these pyrochlore structures have all demonstrated that the water molecules and hydroxyl protons reside within the tunnels.[8,28,29] In addition, Brunauer–Emmett–Teller adsorption measurements have shown that the dehydrated $KTa_2O_5(OH)$ defect pyrochlore maintains its open structure at 300 °C, while *in situ* hot stage XRD in this study and by others[27] have shown that the crystal structure is stable to at least 400 °C. Using *in situ* diffuse reflectance FTIR, Duan *et al*. observed that heating the defect pyrochlore powder up to 250 °C caused an almost complete disappearance of the bending vibrations of H_2O at 1600–1650 cm^{-1} although the broad band due to O–H stretching was still present.[8] As such, the contraction of the pyrochlore lattice upon heating, as observed by *in situ* hot stage XRD in this study, is largely due to the loss of molecular water from the channels, which, upon readsorption at room temperature, leads to an expansion of the lattice.

The driving force for adsorption of water in molecular sieves is the formation of ion–dipole pairs, in this case between water molecules and potassium ions, and hydrogen bonding between water molecules and oxygen of the B_2O_6 framework (the 48*f* oxygen).[30] The hydrogen bonding between 48*f* oxygen and water molecules reduces the Coulomb attractive forces between ions in the B_2O_6 framework and leads to an expansion of the lattice. This could explain the increased lattice parameters observed for the as-synthesized defect pyrochlore powders. Consequently, the removal of water molecules upon dehydration would then lead to a contraction of the lattice and then expand again when rehydrated, as observed in the *in situ* hot stage XRD experiments. This ready reversibility supports the proposal that physisorbed (e.g., hydrogen-bonded water molecules) rather than chemisorbed (e.g., hydroxyl groups) species are involved in the expansion and contraction of the lattice. The ability of physisorbed water to cause structural changes at room temperature has also been observed for other molecular sieve materials.[31,32]

V. CONCLUSIONS

Potassium tantalate powders were synthesized by the hydrothermal method at 100 to 200 °C in highly alkaline (4 to 15 M), aqueous KOH solutions for periods up to 48 h. A defect pyrochlore, with the approximate formula, $K\square Ta_2O_5(OH)\square \cdot nH_2O$ ($n \approx 1.4$), was the stable composition at 4 M KOH. At higher OH^- concentration, the pyrochlore was only an intermediate phase; the pyrochlore reacted further with KOH to form a defect perovskite phase. At 15 M KOH, no intermediate pyrochlore was formed and a defect perovskite phase, $K_{0.85}Ta_{0.92}O_{2.43}(OH)_{0.57} \cdot 0.15H_2O$, was the stable phase. Both phases contained OH^- ions on oxygen sites and water molecules on vacant potassium and/or oxygen sites. The water molecules easily diffuse to the surface at temperatures <350 °C; for the pyrochlore, the water re-adsorbs from the atmosphere after cooling.

ACKNOWLEDGMENTS

This work was supported by the Materials Research Laboratory program of the National Science Foundation under Award No. DMR00-80034. G.K.L. Goh acknowledges the Institute of Materials Research and Engineering

(Singapore) for the provision of a research scholarship. Dr. Sonjong Hwang of the California Institute of Technology kindly collected the NMR data.

REFERENCES

1. O.G. Vendik, E.K. Hollmann, A.B. Kozyrev, and A.M. Prudan, J. Superconductivity **12,** 325 (1999).
2. H.M. Christen, L.A. Boatner, J.D. Budai, M.F. Chisholm, L.A. Gea, P.J. Marrero, and D.P. Norton, Appl. Phys. Lett. **68,** 1488 (1996).
3. G.K.L. Goh, C.G. Levi, and F.F. Lange, J. Mater. Res. (in press).
4. A.T. Chien, J.S. Speck, F.F. Lange, A.C. Daykin, and C.G. Levi, J. Mater. Res. **10,** 1784 (1995).
5. A.T. Chien, J.S. Speck, and F.F. Lange, J. Mater. Res. **12,** 1176 (1997).
6. A. Reisman, F. Holtzberg, M. Berkenblit, and M. Berry, J. Am. Chem. Soc. **78,** 4514 (1956).
7. S. Hirano, T. Yogo, K. Kikuta, T. Morishita, and Y. Ito, J. Am. Ceram. Soc. **75,** 1701 (1992).
8. N. Duan, Z-R. Tian, W.S. Willis, S.L. Suib, J.M. Newsam, and S.M. Levine, Inorg. Chem. **37,** 4697 (1998).
9. Powder Diffraction Files, Card No. 35-1464 (Joint Committee on Powder Diffraction Standards, Swarthmore, PA, 1992).
10. Powder Diffraction Files, Card No. 38-1470 (Joint Committee on Powder Diffraction Standards, Swarthmore, PA, 1992).
11. E. Brunner, H.G. Karge, and H. Pfeifer, Z. Phys. Chem. **176,** 173 (1992).
12. S.Q. Fu, W-K. Lee, A.S. Nowick, L.A. Boatner, and M.M. Abraham, J. Solid State Chem. **83,** 221 (1989).
13. A.T. Chien, X. Xu, J.H. Kim, J.S. Speck, and F.F. Lange, J. Mater. Res. **14,** 3330 (1999).
14. D. Hennings and S. Schreinemacher, J. Eur. Ceram. Soc. **9,** 41 (1992).
15. S. Wada, T. Suzuki, and T. Noma, J. Ceram. Soc. Jpn. **104,** 383 (1996).
16. E-W. Shi, C-T. Xia, W-Z. Zhong, B-G. Wang, and C-D. Feng, J. Am. Ceram. Soc. **80,** 1567 (1997).
17. M.T. Weller and P.G. Dickens, J. Solid State Chem. **58,** 164 (1985).
18. S. Wada, T. Suzuki, and T. Noma, Jpn. J. Appl. Phys. **34,** 5368 (1995).
19. R. Waser, Z. Naturforsch. **42a,** 1357 (1987).
20. K.D. Kreuer, St. Adams, W. Münch, A. Fuchs, U. Klock, and J. Maier, Solid State Ionics **145,** 295 (2001).
21. A-J. Li and R. Nussinov, Prot. **32,** 111 (1998).
22. R.D. Shannon and C.T. Prewitt, Acta Crystall. B**25,** 925 (1969).
23. A.W. Sleight, Inorg. Chem. **7,** 1704 (1968).
24. M.A. Subramanian, G. Aravanudan, and G.V. Subba Rao, Prog. Solid State Chem. **15,** 55 (1983).
25. J. Pannetier, J. Phys. Chem. Solids **34,** 583 (1973).
26. J.B. Goodenough, H.Y-P. Hong, and J.A. Kafalas, Mater. Res. Bull. **11,** 203 (1976).
27. N. Kumada, N. Ozawa, N. Kinomura, and F. Muto, Mater. Res. Bull. **20,** 583 (1985).
28. P.G. Dickens and M.T. Weller, Solid State Comm. **59,** 569 (1986).
29. M.A. Butler and R.M. Biefeld, Phy. Rev. B **19,** 5455 (1979).
30. K. Seff, in *Recent Advances and New Horizons in Zeolite Science and Technology,* Stud. Surf. Sci. Catal. **102,** edited by H. Chon, S.I. Woo, and S-E. Park (1996), p. 267.
31. N.J. Tapp, N.B. Milestone, M.E. Bowden, and R.H. Meinhold, Zeolites **10,** 105 (1990).
32. T.M. Nenoff, J.B. Parise, G.A. Jones, L.G. Galya, D.R. Corbin, and G.D. Stucky, J. Phys. Chem. **100,** 14256 (1996).